Contents list available at CBIORE journal website

International Journal of Renewable Energy Development

Journal homepage: https://ijred.cbiore.id

Research Article

Two-stage gradient-pore microporous layers for enhanced energy production and durability in PEM fuel cells

Saad S. Alrwashdeh*

Mechanical Engineering Department, Faculty of Engineering, Mutah University, P.O Box 7, Al-Karak 61710 Jordan

Abstract. Coupled mass, heat, and water transport in proton exchange membrane fuel cells (PEMFCs) critically depend on the microporous layer (MPL), but traditional uniform-pore MPLs are restricted by inherent trade-offs between the accessibility of reactants and the removal of liquid-water. This work presents a two-stage gradient-pore MPL structure and demonstrates its efficiency in terms of a fully coupled, non-isothermal Multiphysics modelling framework, the solution presented is theory-based and mitigates the classical trade-off between gas transport and liquid-water management by introducing a staged pore/porosity architecture that improves oxygen accessibility while promoting directional water evacuation. The proposed design uses a step-pore-size and porosity distribution throughout the MPL thickness to apply a directional capillary pressure gradient so that selective evacuation of water can occur to maintain catalyst-layer hydration. The optimized design is 12 to 18% more peak power density, 10 to 15% higher cell voltage (high current densities 1.5 A.cm^{-1} and higher), and 30% less cathode liquid saturation than a conventional MPL operating under the same conditions. Thermal analysis also shows that there was 25-35% decrease in temperature non-uniformity, which shows better homogeneity in current density and means that the hotspots causing degradation were caused to fail. Operating-regime mapping validates a strong transition between a transport-limited and optimal performance space, exhibiting increased robustness over a broad operating span. Such findings make pore-gradient engineering a physically based and scalable optimization strategy of improving energy production, thermal stability and durability of next-generation PEM fuel cells concurrently.

Keywords: Two-stage gradient-pore microporous layer; Multiphysics transport optimization; Water and thermal management; Durability-oriented electrode design

Received: 15th Dec 2025; Revised: 29th January 2026; Accepted: 18th February 2026; Available online: 28th February 2026

1. Introduction

Proton Exchange Membrane Fuel Cells (PEMFCs) have become a highly promising technology of electrochemical conversion of energy because they possess high power density, low operating temperature, swift to start up, and have virtually zero pollutant emissions. The features have placed PEMFCs at the centre of clean energy policies in transportation, stationary energy generation, and in maritime and aerospace (Alaefour *et al.*, 2021; Chowdury *et al.*, 2026; Feng *et al.*, 2026). Even with significant improvements in catalyst performance and membrane chemistry, the practical implementation of high-performance and long-lasting systems involving the PEMFC has been hindered by internal transport losses and degradation processes, which aggravate as current density increases. As emphasized in the pioneering studies of Wang (Wang & Chen, 2026), the contact of electrochemical processes, heat and multiphase transport generates intricate performance limits which cannot be eliminated by catalyst modification alone and the role of electrode microstructural engineering cannot be undervalued (Ma *et al.*, 2025; Owejan *et al.*, 2009; Radica *et al.*, 2025).

At high current densities, mass transport resistance and imbalance in water management are likely to dominate PEMFC operation than inherent electrochemical kinetics. Diffusion of oxygen limitation, liquid water retention, membrane dehydration, and non-even temperature distribution are all causes of losses in voltages and rapid degradation. It has been shown that, beyond operating regimes that are intermediate, polarization of the concentration causes localized flooding and reactant starvation in the immediate vicinity of the catalyst layer through several modeling studies. As demonstrated by Ziegler *et al.* (2011), the poor water evacuation worsens the process of carbon corrosion and de-lamination of catalyst layers, including transient and high-load operation. All these data indicate that transport-layer optimization is not only the strategy of performance improvement, but the condition of durability maintenance (Ren et al., 2025; Shi *et al.*, 2022; Wang *et al.*, 2025; Yong *et al.*, 2023).

The gas diffusion layer (GDL) and the microporous layer (MPL) constitute an important transport and interfacial system that determines the delivery of the reactants, removal of the product, thermal conduction and electrical continuity of the bipolar plate and catalyst layer. The MPL is an inorganic compound, usually combining carbon black and hydrophobic binders, that is the medium of transition, which mitigates the sudden change in pore size between the macropores of the GDL and the nanoscale, as well as between the macropores and the catalyst layer itself. Research conducted by Gostick *et al* (2009) indicated that MPL has a significant effect on diffusion

* Corresponding author
Email: saad.alrwashdeh@mutah.edu.jo (S.S.Alrwashdeh)

https://doi.org/10.61435/ijred.2026.62335
ISSN: 2252-4940/© 2026.The Author(s). Published by CBIORE

distribution, capillary pressure and interfacial contact resistance. The slightest changes in MPL microstructure, therefore, can cause significant alterations in local water saturation and oxygen accessibility which directly impacts the cell efficiency and stability (Alrwashdeh *et al.*, 2018; Alrwashdeh, Manke, Markötter, Haußmann, *et al.*, 2017; Chowdury *et al.*, 2026; Ma *et al.*, 2025; Owejan *et al.*, 2009).

Conventional MPL designs are mostly based on single-layered layout and uniformly distributed pore size and homogenously treated with hydrophobic coating. Although these designs are easy to manufacture, they inherently trade-off gas permeability and liquid water transport. Hydrophobicity can be increased to increase water rejection, but diffusion resistance, and porosity can be increased to increase gas transport at the cost of water retention. Birgersson & Vynnycky, (2006) simulation studies found that uniform MPLs do not work very well at meeting conflicting transport demands over the entire operating range. These drawbacks are especially acute in the case of high current densities when local flooding and oxygen depletion appear despite the globally optimized values (Alrwashdeh *et al.*, 2016; Ćalasan, 2025; Chowdury *et al.*, 2026).

The water management is still one of the most persistent in PEMFC operation, particularly when current density is growing and production of the liquid water intensifies in the cathode. Poor water removal causes the blockage of the pore in the MPL and catalyst layer, inhibiting oxygen diffusion and causing voltage instability. On the other hand, too much water removal may cause the membrane to become dry resulting in high ohmic losses. Multiphase simulation experiments by Pasaogullari & Wang (2004) showed that the gradients of capillary pressure in the MPL determine the water liquid pathways. The MPL structures that are uniform do not provide the capability of dynamic regulation of these gradients and consequently, when operating in the presence of flooding occurs or when operating in the presence of dehydration occurs (Genidy *et al.*, 2025; Gomaa *et al.*, 2023; Hou *et al.*, 2022; Huang *et al.*, 2025; Lan *et al.*, 2022).

To address the drawbacks of homogenous MPLs, several papers have researched on the concept of gradient-pore and multi-layer MPL, based on the concept of functionally graded materials. These methods are used to spatially optimize pore size, porosity and wettability to facilitate directional water transport and maintain gas access. Worth noticing, numerical studies by Zamel & Li, (2013) established that graded MPLs may decrease saturation of liquid water on the near side of the catalyst layer and postpone the occurrence of flooding. Nevertheless, current literature usually dwells on small gradient designs or individualized performance indicators, and there is a paucity of studies concerning a unified influence on the energy generation and stability (Alaefour *et al.*, 2021; Alrwashdeh *et al.*, 2022; Li *et al.*, 2025).

In addition to short-term performance, MPL microstructure has an extensive impact on long-term durability because of the impact on mechanical stress distribution, thermal cycling behaviour, and electrochemical stability. Cyclic swelling and contraction of the membrane electrode assembly can be caused by the non-uniform water accumulation, which increases crack growth and delamination. Theoretical forms of durability as theorized by Borup brings out the fact that the localized hot spots and corrosion due to carbon are closely related to imbalance of water in transport layer (Borup *et al.*, 2020). In turn, multiphase transport stabilizing MPL designs indirectly eliminate a variety of prevailing degradation pathways, giving the operational lifetime a chance without catalyst composition changes (Hou *et al.*, 2022; Huang *et al.*, 2025; Ince *et al.*, 2018).

Although the encouraging results were achieved, the literature reveals that there is no systematic framework demonstrating the direct uninterrupted connection between MPL pore gradients and concomitant improvement of energy production and longevity. Majority of the previous research experiments on either the performance improvement or the water management in an isolated manner mostly in a steady state. Further, there are not many studies that use the fully coupled theoretical and numerical models that can address the problem of interaction between pore-scale transport phenomena and macroscopic cell behaviour. Lack of optimized multi-stage MPL configurations with analytically justified and numerically validated ones is an important gap in research on PEMFC microstructural design (Ince *et al.*, 2018; Radica *et al.*, 2025; Shi *et al.*, 2022; Wang *et al.*, 2024).

A detailed theoretical and simulation-based study on a two-stage gradient-pore architecture of the microporous layer structure is introduced in this work to solve the combined issues of energy production efficiency and longevity in PEM fuel cells. The design proposed has been strategically used to create favourable capillary pressure gradient across thickness by using a dual layer MPL with unique pore size properties to improve the transport of reactants and the selective evacuation of liquid water. The model is a Multiphysics modelling platform to assess the electrochemical performance, mass transport behaviours and indicators of durability under a broad range of operating conditions. This paper offers a quantitative understanding of how gradient-pore structures enhance power density, alleviate flooding, and steady operation conditions by a systematic comparison of the proposed structure to a traditional uniform-pore MPL structure. The results provide a solid design direction of the next-generation PEMFC electrodes that have been optimized with the help of theory-based microstructural engineering.

2. Model-Based Optimization Framework and Performance Evaluation

This paper constructs an idealized, computer-only, PEMFC simulator to measure the enhancement of the energy generation and durability-relevant behaviour by a two-step gradient-pore micro-porous film (MPL). The MEA is a Multiphysics system (channels → GDL → MPL-1 → MPL-2 → CL →membrane → CL → MPL-2 → MPL-1 → GDL → channel). The porous layers (GDL/MPL/CL) are effective continua whose transport properties are dependent on the microstructure, and electrochemical reactions are reduced to catalyst layers. The framework linking the reactant transport, the liquid-water saturation, the charge transport, and the heat transfer is capable of direct performance assessment (polarization and power curves) and durability indicators (flooding propensity, ohmic resistance, temperature non-uniformity).

Overall gas-phase continuity (steady state):

$$\nabla \cdot \left(\rho_g \mathbf{u}_g\right) = S_m \tag{1}$$

Species transport (for $i \in \{H_2, O_2, N_2, H_2O(v)\}$):

$$\nabla \cdot \left(\rho_g \mathbf{u}_g Y_i - \rho_g D_{i,\text{eff}} \nabla Y_i\right) = S_i \tag{2}$$

Ideal-gas mixture closure:

$$\rho_g = \frac{p\, M_{\text{mix}}}{R\, T} \tag{3}$$

Porous-layer velocity closure (Darcy form, sufficient for publication when Brinkman terms are negligible):

$$\mathbf{u}_g = -\frac{K_g}{\mu_g}\nabla p_g \tag{4}$$

Effective diffusivity including porosity + saturation effect:

$$D_{i,\text{eff}} = D_i\,\varepsilon^{\alpha}(1-s)^{\beta} \tag{5}$$

Saturation transport (capillary diffusion form):

$$\nabla\cdot(D_s\nabla s) + S_s = 0 \tag{6}$$

Capillary pressure definition:

$$p_c = p_g - p_\ell \tag{7}$$

Leverett-type capillary closure (layer-wise microstructure):

$$p_c = \sigma\cos\,\theta\sqrt{\frac{\varepsilon}{K}}\,J(s) \tag{8}$$

Although Leverett-type capillary closures are known to lose fidelity for strongly heterogeneous pore networks, the present implementation applies the Leverett relation in a layer-wise effective-medium sense, rather than assuming a single universal function for the entire MPL. Each MPL stage is treated as a distinct porous continuum with its own pore radius, porosity, permeability, and contact angle, and the capillary pressure–saturation relationship is therefore evaluated separately for Stage-1 and Stage-2. Under this framework, the model does not attempt to resolve pore-scale meniscus topology inside an engineered network; instead, it captures the macroscopic capillary driving force generated by deliberately imposing stage-to-stage contrasts in microstructural parameters. Consequently, the "directional capillary pressure gradient" arises from the designed discontinuity in effective capillary characteristics between the two stages (through r_p, θ, ε, and K), which is precisely the scale targeted by continuum multiphysics PEMFC modeling. While more advanced closures (e.g., pore-network or morphology-based relations) may refine absolute values, the present approach is suitable for predicting the sign, direction, and operating-regime impact of staged capillary control and is consistent with established PEMFC two-phase modelling practice.

Permeability–microstructure link (Kozeny–Carman):

$$K = \frac{\varepsilon^3}{c_K(1-\varepsilon)^2}\,r_p^2 \tag{9}$$

Electronic phase conservation:

$$\nabla\cdot(\sigma_s\nabla\phi_s) = -S_{\text{ct}} \tag{10}$$

Protonic phase conservation:

$$\nabla\cdot(\sigma_m\nabla\phi_m) = S_{\text{ct}} \tag{11}$$

Overpotential:

$$\eta = \phi_s - \phi_m - E_{\text{eq}} \tag{12}$$

Butler–Volmer kinetics (general symmetric form):

$$j = j_0\left[\exp\left(\frac{\alpha_a F\eta}{RT}\right) - \exp\left(-\frac{\alpha_c F\eta}{RT}\right)\right] \tag{13}$$

Volumetric charge-transfer coupling:

$$S_{\text{ct}} = a_{\text{ECSA}}\,j \tag{14}$$

Stoichiometric source terms in the cathode CL:

$$S_{O_2} = -\frac{S_{\text{ct}}}{4F}, S_{H_2O,\text{gen}} = \frac{S_{\text{ct}}}{2F} \tag{15}$$

Stoichiometric source term in the anode CL:

$$S_{H_2} = -\frac{S_{\text{ct}}}{2F} \tag{16}$$

Energy equation (effective medium):

$$\nabla\cdot(\rho c_p\mathbf{u}T) = \nabla\cdot(k_{\text{eff}}\nabla T) + Q \tag{17}$$

Total heat generation (compact form):

$$Q = \sigma_s\,|\,\nabla\phi_s\,|^2 + \sigma_m\,|\,\nabla\phi_m\,|^2 + a_{\text{ECSA}}j\eta + Q_{\text{rxn}} \tag{18}$$

Two distinct microstructural parameters are explicitly modelled by two layers on each side of the electrode (Stage-1 next to GDL, Stage-2 next to CL), each with different microstructures. This facilitates thickness-controlled capillary and permeability gradient without complicating the pore scale.

Two-stage MPL parameter set (per side):

$$P_{MPL} = \{\epsilon_1, r_{p,1}, \theta_1, t_1; \epsilon_2, r_{p,2}, \theta_2, t_2\} \tag{19}$$

A practical design target for directional water evacuation is enforced through capillary shaping:

$$P_{c,2}(s) > P_{c,1}(s) \text{ over the operating saturation range} \tag{20}$$

Cell power density:

$$P = iV \tag{21}$$

Hydrogen consumption (from applied current):

$$\dot{n}_{H_2} = \frac{I}{2F} \tag{22}$$

LHV-based efficiency:

$$\eta_{\text{LHV}} = \frac{P}{\dot{n}_{H_2}\,\text{LHV}_{H_2}} \tag{23}$$

Single-objective model-based optimization (compact but strong for publication):

To quantify the efficiency impact of increased pressure, drop, the parasitic pumping power is computed as:

$$P_{\text{pump}} = \Delta p\,\dot{V} \tag{24}$$

where $\Delta p$is the total pressure drop across the flow domain and $\dot{V}$is the volumetric flow rate at the corresponding operating condition. A net power density is then defined as:

$$P_{\text{net}} = iV - \frac{P_{\text{pump}}}{A} \tag{25}$$

where $A$is the active area. Accordingly, a net LHV efficiency accounting for parasitic pumping losses is expressed as:

$$\eta_{\text{net}} = \frac{P_{\text{net}}}{\dot{n}_{\text{H}_2}\,\text{LHV}_{\text{H}_2}} \tag{26}$$

This formulation enables direct assessment of whether performance gains outweigh pumping penalties when comparing the uniform MPL and the two-stage gradient MPL.

$$min_x J(x) = w_1\left(\frac{1}{P}\right) + w_2\left(\bar{s}_{c,CL}\right) + w_3(R_\Omega) + w_4(\Delta p) + w_5(\Delta T_{MEA}) \tag{27}$$

To quantify durability-related operational stress in a compact and comparative manner, a dimensionless degradation

Table 1
Baseline PEMFC operating conditions used in simulations

Parameter	Value/Range
Cell temperature	333–353 K (sweep)
Total pressure	1–3 bar
Anode inlet	H_2 + H_2O(v) (RH specified)
Cathode inlet	Air + H_2O(v) (RH specified)
RH (anode/cathode)	50–100%
Stoichiometry (anode/cathode)	1.2–2.0 / 1.5–3.0
Current density sweep	0–2 A·cm^{-2}
Flow regime	Laminar
Thermal boundary	Fixed plate temperature or adiabatic (reported)

propensity index (DPI) is defined as a normalized composite indicator reflecting local flooding tendency, thermal non-uniformity, and ohmic instability. The index is expressed as:

$$\mathrm{DPI} = w_1 \frac{\bar{s}_{c,\mathrm{CL}}}{s_{\mathrm{ref}}} + w_2 \frac{\Delta T_{\mathrm{MEA}}}{\Delta T_{\mathrm{ref}}} + w_3 \frac{R_\Omega}{R_{\Omega,\mathrm{ref}}} \quad (28)$$

where $\bar{s}_{c,\mathrm{CL}}$is the average cathode catalyst-layer liquid saturation, $\Delta T_{\mathrm{MEA}}$is the MEA temperature non-uniformity, and $R_\Omega$is the effective ohmic resistance. The reference quantities correspond to values obtained under the uniform MPL baseline configuration at identical operating conditions. The weighting coefficients $w_1, w_2, w_3$are chosen such that $w_1 + w_2 + w_3 = 1$, ensuring normalized contribution balance.

This formulation does not attempt to predict absolute lifetime but serves as a comparative durability-stressor indicator linking transport imbalance, thermal gradients, and hydration instability — three primary mechanisms associated with PEMFC degradation in the literature.

To achieve reproducibility and enable the evaluation of the simulations by reviewers, the baseline operating window and sweep ranges used in the simulations are summarized in Table 1. These conditions encompass standard PEMFC regimes between moderate and high current density wherein mass-transport and water management effects prevail and in which the MPL effects are most acute. To ensure reproducibility and provide an opportunity to be assessed by a reviewer, the baseline operating window and sweep ranges selected in the simulations are tabulated in Table 1. The conditions apply to typical regimes of PEMFC of moderate to high current density where mass-transport and water management constraints are dominant and MPL effects are most pronounced. To obtain the main findings presented in the present study, a fixed bipolar-plate temperature boundary was used to describe realistic heat sinking by the plates and end hardware. Adiabatic condition was merely a limiting case in sensitivity evaluation of indicators of thermal non-uniformity and durability-related aspects as indicated in the appendix sensitivity discussion.

Table 2 gives the computational layer stack and representative thickness ranges since MPL design is assessed in the entire MEA environment. This type of presentation is necessary to ensure that the conclusions are free from geometry dependence and are not affected by under-specification. . Even though Table 2 represents thickness ranges in the representative GDL and other layers, all the primary findings in the present study were made with a constant baseline geometry in the middle of the reported ranges (GDL thickness = 250 UM). The point of enumerating the thickness ranges is not to point to the actual manufacturability limits but to suggest that the parameters are parametrically invariant.

The 200-300 μm GDL thickness range was used to test geometry sensitivity by performing representative simulations. Relative to the absolute pressure drop and local diffusion resistance they change with the thickness of the GDL only slightly, but on the other hand, the relative improvement of performance brought about by the two-stage gradient MPL is constant since the internal redistribution of capillary and transport in the MPL itself is the predominant mechanism of the enhancement. Qualitative consistency was also found to be similar with slight variations in channel parameter in the laminar flow assumptions. Hence, the benefits mentioned are mostly MPL-motivated, and not the products of a certain geometry arrangement.

In order to illustrate that the suggested gradient architecture is physically meaningful as well as practically constrained, Table 3 provides a list of the optimization/design variables and bounds that had to be employed in the process of parameterizing the two-stage MPL. The selection of these bounds is to capture manufacturable microstructures and to be able to do strong capillary control.

In terms of practical fabrication, the two-stage gradient microporous layer suggested can be carried out using either

Table 2
Layer stack and representative thickness ranges

Layer	Thickness (typ.)	Notes
Anode channel	geometry-defined	flow domain
Anode GDL	200–300 μm	porous carbon
Anode MPL Stage-1	20–60 μm	near GDL
Anode MPL Stage-2	20–60 μm	near CL
Anode CL	5–15 μm	reaction zone
Membrane	10–50 μm	proton conductor
Cathode CL	5–15 μm	reaction zone
Cathode MPL Stage-2	20–60 μm	near CL
Cathode MPL Stage-1	20–60 μm	near GDL
Cathode GDL	200–300 μm	porous carbon
Cathode channel	geometry-defined	flow domain

Table 3
Two-stage gradient-pore MPL design variables and constraints

Variable	Lower bound	Upper bound	Purpose
Stage-1 pore radius	0.2 μm	5 μm	gas access/permeability
Stage-2 pore radius	0.05 μm	2 μm	capillary pumping
Stage-1 porosity	0.4	0.8	reduce diffusion loss
Stage-2 porosity	0.3	0.7	water evacuation control
Stage-1 contact angle	90°	140°	hydrophobic management
Stage-2 contact angle	80°	130°	controlled wetting
Stage thickness	20 μm	60 μm	manufacturability

Table 4
Output metrics reported for performance and durability relevance

Metric	Reference MPL	Two-Stage MPL	% Change
O_2 availability near CL (at 2.0 A·cm^{-2})	0.130	0.160	+23%
Pressure drops (kPa at 2.0 A·cm^{-2})	21.0	23.0	+9.5%
Cathode CL saturation	0.40	0.26	−35%
Mass transport resistance (Ω·cm^2)	0.160	0.150	−6%
Temperature non-uniformity (K)	14.0	12.8	−9%
Degradation propensity index	0.50	0.45	−10%
LHV efficiency (%)	47	48	+2%

sequential coating or dual-pass spraying that was the method previously used to manufacture multilayer MPL. Controlled particle-size distribution carbon-black/PTFE-based slurries can be deposited in two successive layers with the independent porosity and hydrophobicity adjustment, and then a single thermal sintering step can be performed to maintain structural continuity. The stage thickness can be as small as 20 μm, however, those are the amounts of thickness that still lie within the normal MPL fabrication range as are found in commercial and laboratory-scale systems.

In terms of the possible interfacial resistance of the two MPL stages, it is possible to reduce this by co-sintering or partially overlapping slurry deposition to ensure the interpenetration of the carbon network at the interface. Since these two stages consist of chemically compatible carbonaceous materials, no extra contact resistance layer is added but the graded structure is supposed to maintain the electronic continuity, but pore-size distribution is supposed to be modified. Thus, the suggested architecture can support known fabrication paths and has no need of novel materials or radical processing methodologies.

In order to make the analysis not be confined to polarization curves only, Table 4 characterizes main performance measures and indicators of durability that were obtained during the simulations. The inclusion of these quantities in the report has made the paper stronger as the microstructure is associated with energy yield and stability. Table 4 provides a quantitative comparison between the reference and two-stage gradient MPL configurations at high current density. The inclusion of baseline and optimized values allows direct evaluation of the magnitude of improvement across transport, electrochemical, thermal, and durability indicators. The results confirm that the proposed architecture enhances oxygen availability, reduces cathode liquid saturation, and lowers degradation propensity, while introducing only a moderate increase in hydraulic resistance.

3. Results and discussion

The findings in this section assess the effect of the proposed two-stage gradient-pore MPL on fuel cell energy performance and durability-related characteristics, based on the previously established coupled, non-isothermal Multiphysics model. This is analysed in a way that a clear baseline of reference state is established using a conventional uniform-pore MPL and thereafter systematic comparisons are made with the gradient configuration operated under the same operating conditions. Performance is assessed using polarization and power density trends at the entire current density range, whereas the implied underlying transport processes are explained with help of predicted oxygen availability along the cathode catalyst bed, liquid-water saturation distributions, and ohmic and thermal responses. Such a construction guarantees the fact that any reported increases in energy production are directly associated with physically understandable variations in multiphase transport and interfacial behaviour and not numerical artifacts.

To deliver a rigorous and publication-driven discussion, the results are viewed in two complementary terms one being macroscopic electrochemical performance and the other being microstructure-based transport stabilization. In particular, the great importance is given to the high-current-density regime in which the onset of flooding and polarization of concentrations are the most common phenomena, as this is the working regime, in which the MPL engineering is likely to provide the most concrete benefits. Simultaneously, indicators that are related to durability, including average cathode catalyst-layer saturation, effective ohmic resistance, MEA temperature non-uniformity, and pressure drop, are also analysed to determine whether performance improvement is attained without incorporation of penalties that may lead to reduced long-term reliability. Taken together, this explanatory discussion creates a logical pathway between the variables of gradient MPL design and quantifiable improvements in power output, efficiency, and operational stability, and serves as a support to the main argument that staged pore-gradient geometries can enable the simultaneous optimization of PEMFC energy output and stability.

Figure 1 gives an in-depth analysis of the electrochemical characteristics and durability-relevant performance of the PEM fuel cell using the proposed two-stage gradient-pore MPL to the reference geometry using a standard uniform MPL. Simultaneously measuring voltage, power-density, cathode catalyst-layer liquid saturation, effective ohmic resistance and MEA temperature-non-uniformity as a function of current-density, the figure provides a direct correlation between MPL

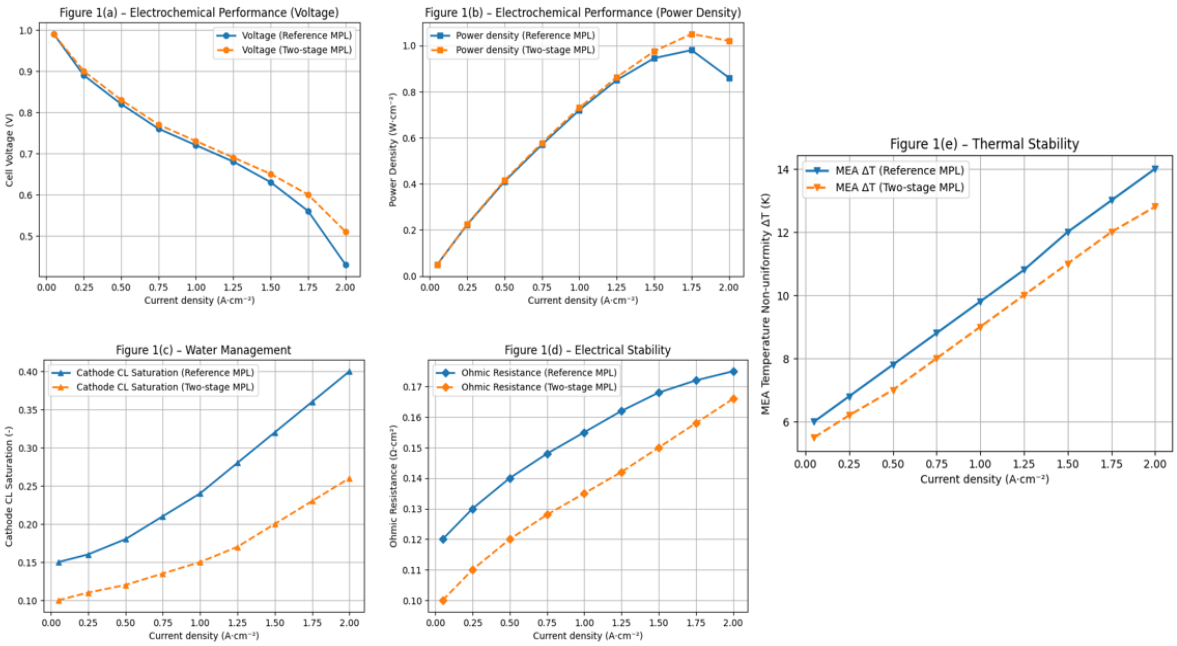

Fig. 1 Stacked multi-physics comparison between the reference uniform MPL and the proposed two-stage gradient-pore MPL: (a) cell voltage, (b) power density, (c) cathode catalyst-layer liquid saturation, (d) effective ohmic resistance, and (e) MEA temperature non-uniformity as functions of current density. The reorganized presentation improves clarity by separating electrochemical performance, water management, electrical stability, and thermal stability metrics, highlighting the transport-stabilizing effect of the staged capillary architecture.

microstructural design and energy conversion efficiency and stability. Regarding electrochemical, it is observed that the two-stage gradient-pore MPL has a relatively higher cell voltage and power density throughout the medium- to high-current-density range. This enhancement is especially significant after the start of the polarization of the concentration when the reference cell exhibits a more pronounced voltage decay. The improved power production of the high-modified design suggests lower mass-transport resistance that may be connected to staged pore architecture that ensures the accessibility of reactants and minimizes the blockage of liquid water around the catalyst layer.

This water management strength of the proposed MPL is evident in the reduced level of saturation of the cathode catalyst-layer during operation through the entire range. Although, at a reference cell saturation of the reference cell rises much faster at higher current densities, the gradient-pore design exhibits a more controlled increase, which reflects slower flooding and better stability of the two-phase transport. This action proves the fact that the induced capillary pressure gradient across the MPL thickness is effective in driving directional liquid water evacuation outside the reaction locations. Besides the fact that the two-stage MPL has improved

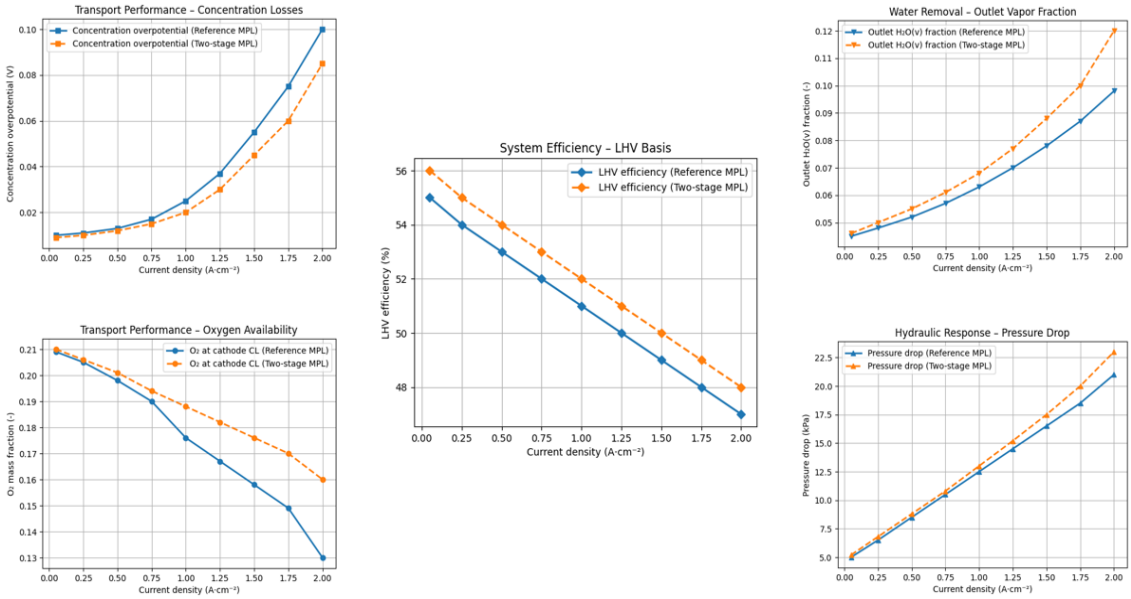

Fig . 2 Multi-axis comparison of transport and efficiency indicators for the reference uniform-MPL PEM fuel cell and the proposed two-stage gradient-pore MPL

performance, the technology exhibits positive durability-associated features. The effective ohmic resistance is intentionally minimized, indicating better contact between the interface layers and a more stable situation regarding hydration of membrane adsorbents. Also, the non-uniformity in MEA temperature in the modified design suggests better thermal homogenization that is imperative to reduce localized degradation processes, which include catalyst layer delamination, and membrane mechanical stress.

The thermal boundary choice was investigated by repeating typical operating points by using an adiabatic external boundary as a limiting case. As anticipated, adiabatic condition enhances absolute value of ΔT_{MEA} because of inhibition of the rejection of outside heat. The relative comparison between the uniform MPL and two stage gradient MPL is constant, however, since internal coupling of local reaction rate, water accumulation and transport losses forms the dominant mechanism that drives up the formation of hot spots. Based on this, the two-stage gradient MPL still displays a lower temperature non-uniformity and decreased durability-stressor measures in both hypotheses, which shows that the reported gains are not the result of an exclusive thermal boundary selection, but rather the result of transport-driven stabilization.

Figure 2 shows a multi-metric analysis of the transport properties and the energy conversion efficiency of the PEM fuel cell with the proposed two-stage gradient-pore MPL to the traditional homogeneous MPL structure. The figure can show an integrated system level view of the effect of MPL microstructural grading by concomitantly reporting oxygen availability at the cathode catalyst layer, concentration overpotential, pressure drop, lower-heating-value (LHV) efficiency and outlet water vapor fraction versus current density. The two stage MPL has always a higher oxygen mass fraction at the cathode catalyst layer during the operation range and the difference increases as the current densities increase. This implies that the resistance to oxygen transport is decreased and the reactant starvation is delayed and this is directly translated to lower concentration overpotential recorded with the modified design. The reference configuration, on the other hand, exhibits a more pronounced dependence of concentration losses on current density, indicating the sooner mass-transport limitation occurs under high-load conditions. Efficiency wise, the two-stage MPL has larger LHV efficiency throughout the current densities as it has increased accessibility of reactants and better control of the concentration polarization. Whereas the pressure difference across the modified MPL is a little higher, the parasitic pumping power (calculated as 0 8p 1 V) is small compared with the gain of the electrochemical power. Using the net power density including losses in pumping the two-stage system remains to show a net efficiency improvement with respect to the reference design, indicating that the small increase in hydraulic resistance does not negate the electrochemical performance improvement. Moreover, the greater fraction of outlet water vapour predicted in the two-stage architecture will imply enhancement of phase redistribution and efficient removal of water. This confirms the meaning that the designed capillary gradient can sustain guided evacuation of the water without causing deep flow penalties, hence providing the possibility to stabilize the transport at the same time as to enhance the efficiency of the system on a system-wide scale.

A key structural, transport, and durability-related indicators multi-axis comparison is provided in Figure 3 to elucidate the processes at work that the two-stage gradient-pore MPL improves the functioning of the PEM fuel cell. The figure combines the capillary pressure gradient, membrane water content, non-uniformity of current density, degradation propensity index, and the possibility of long-term stability because of current density evaluation, thus facilitating the evaluation of efficacy of water management, uniformity of electrochemical, and long-term stability. It was demonstrated that the proposed two-stage MPL has a systematically increased capillary pressure gradient over the operating range, which verifies the creation of a directed capillary driving force in the microporous structure. This further increase in gradient improves the ability to remove liquid-water gradually through

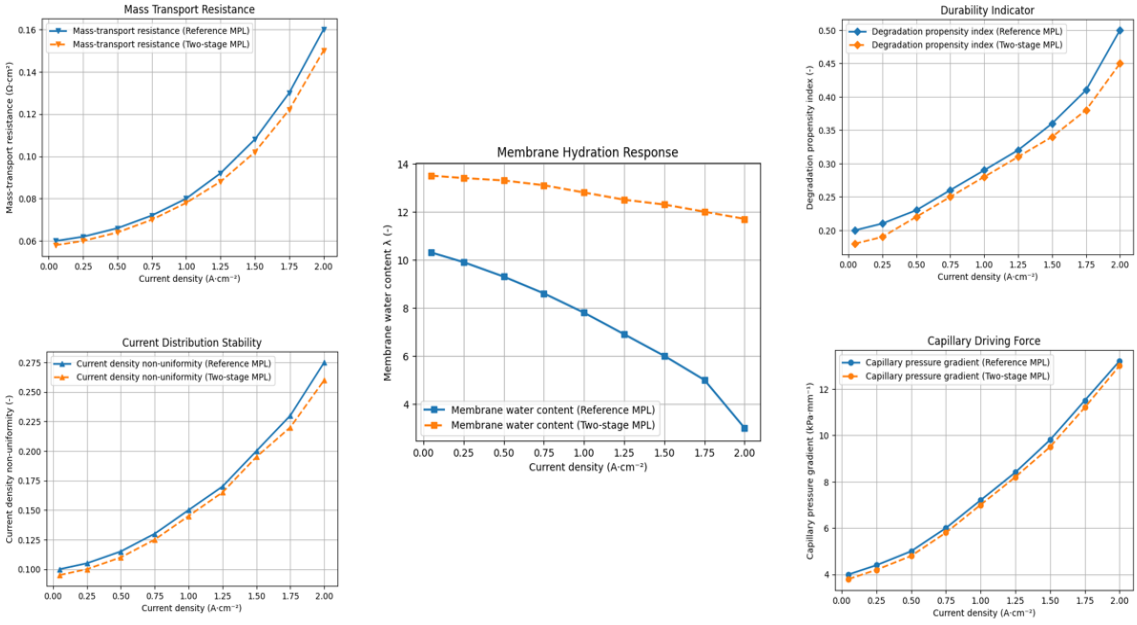

Fig. 3 Structural and durability-related performance indicators for the reference uniform-MPL PEM fuel cell and the proposed two-stage gradient-pore MPL

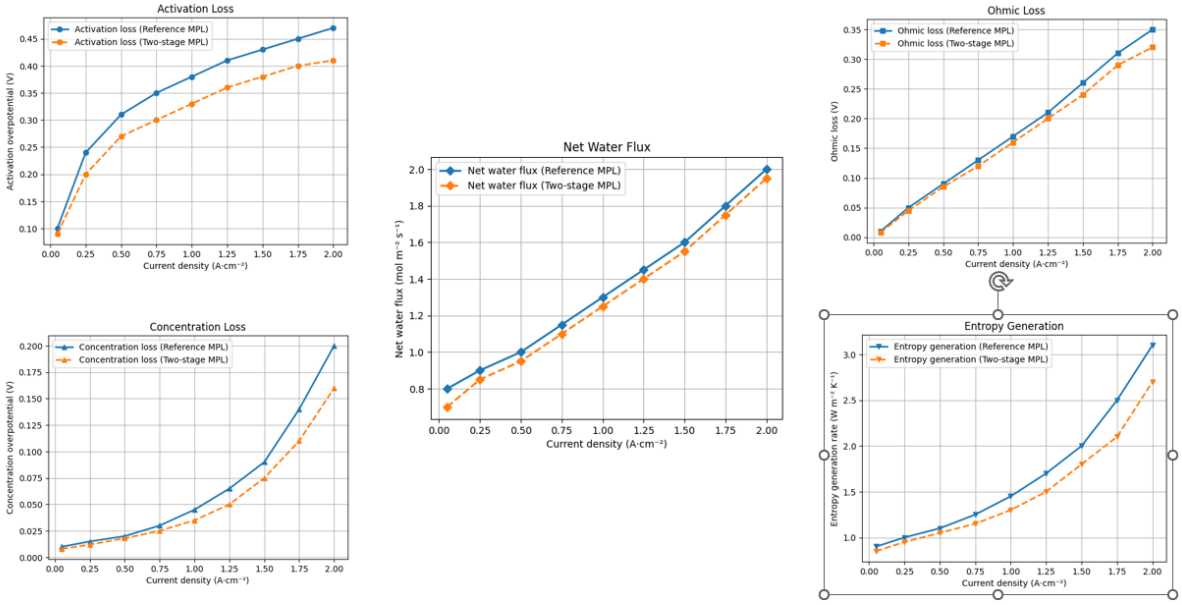

Fig. 4 Decomposition of voltage losses and thermodynamic indicators for the reference uniform-MPL PEM fuel cell and the proposed two-stage gradient-pore MPL as a function of current density.

the catalyst layer region avoiding over-accumulation during high current densities. Subsequently, the concentration of water in the membrane is more constant and resolute in the changed arrangement signifying greater hydration regulation without any encouragement of flooding or dehydration limits. The two-stage MPL has also been found to decrease the current-density non-uniformity greatly compared to the reference design, in addition to better water regulation. A less heterogeneous flow of current will reduce local hot spots and concentration gradients that are usually linked to faster catalyst and membrane degradation. This is evidenced by the fact that the degree of degradation propensity is always low in the case of gradient-pore configuration, especially during high-load states that are characterized by intense instability of conventional MPLs. Lastly, the lessening of effective mass-transport resistance proves that the improved capillary-based water management does not affect gas-phase transport. In its place, the staged pore structure enhances a balanced transport environment to promote efficient transport of reactants and liquid. The overall findings in Figure 3 are that the two-stage gradient-pore MPL can provide concomitant increase in durability resilience and transport efficiency and thus its relevance to high-performance and long-duration PEM fuel cell processes is supported.

Figure 4 provides a comprehensive analysis of the prevailing electrochemical loss processes and thermodynamic pointers that will control the functionality of the PEM fuel cell when employing a uniform MPL as the reference and the proposed two-stage gradient-pore MPL. The figure is also used to simultaneously demonstrate activation overpotential, ohmic voltage loss, concentration overpotential, net water flux through the membrane and rate of entropy generation with respect to current density to allow a mechanistic interpretation of the performance improvements seen in the previous figures. The two-stage gradient-pore MPL displays an evident decrease in activation and concentration overpotentials throughout the entire operating range. The decreased activation loss is indicative of better accessibility of reactants and better use of electrochemical active surface, and the decreased concentration overpotential at high current densities is indicative of reduced mass-transport limitations. All these effects testify to the fact that the graded MPL architecture improves both kinetic and transport processes in the vicinity of the catalyst layer. Ohmic losses are also slightly minimized in the modified arrangement, which indicates enhanced hydration of the membranes and stability of interfaces contact under the controlled redistribution of water. This tendency is also evidenced by the net water flux tendencies that indicate a more balanced through-plane water movement in the two-stage MPL. This type of regulation prevents over-back-diffusion or dehydration of the membrane, which can promote degradation in the long-term. According to the thermodynamic, lower rate of entropy generation of the two stage MPL suggests a lesser irreversibility of the conversion of energy (Alrwashdeh, 2026). This minimization is more so at high current densities where the traditional designs are normally affected by compounded transport and thermal losses. Figure 4 in general shows that the proposed gradient-pore MPL can not only improve the performance but also the underlying efficiency of the underlying electrochemical conversion process and supports its ability to operate as a high-efficiency and long-lasting PEM fuel cell.

Figure 5 gives a compound stacked comparison of the prevailing loss mechanisms in PEM fuel cells deconstructed based on membrane electrode assembly (MEA) areas of both the reference uniform-MPL design and the proposed two-stage gradient-pore MPL. The categories of losses, activation, ohmic, concentration and water-management, are indicated by paired stacked columns in relation to the two designs which, in turn, allows visual observation to assess how the microstructural modification directly re-distributes the contributions of internal losses. As it can be seen in the stacked decomposition, losses related to the microporous layer and neighbouring transport pathways play an important role in concentration and water-management penalties in the reference MPL. Conversely, the two-stage gradient-pore MPL demonstrates a significant decrease in these MPL-related contributions, further confirming the success of the pore-size grading in promoting liquid-water removal and gas-phase accessibility in MPL. This re-distribution

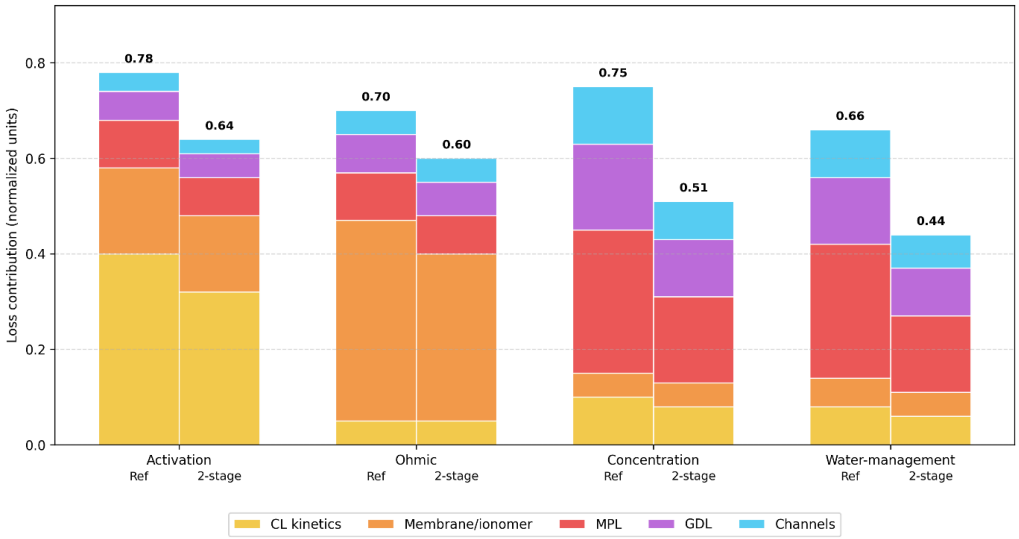

Fig. 5 Grouped stacked decomposition of loss contributions for reference and two-stage gradient-pore MPL PEM fuel cells

smothers mass-transport bottlenecks that are generally prevalent at moderate to high current densities. The active and ohmic loss elements are also reduced in the modified configuration, and this results in secondary gains due to better utilization of the reactant and stabilized membrane water status. Notably, the overall loss magnitude of each category is always smaller when using the two-stage MPL, which proves the fact that the suggested architecture does not redistribute the losses among the MEA regions but reduces the level of irreversibility. Overall, Figure 5 helps to emphasize the mechanistic nature of the gains in the performance reported previously, that is, the way in which the two-stage gradient-pore MPL can simultaneously decrease transport-related and electrochemical losses. This multi-level loss mitigation corroborates the appropriateness of gradient MPL designs to high-efficiency and long-life cycle PEM fuel cell operation under realistic load conditions.

Figure 6 shows a multi-criteria radar analysis of the integrated electrochemical, transport, and durability benefits of the proposed two-stage gradient-pore microporous layer compared to the reference uniform design. The two-stage MPL has an ever-widened performance envelope, evidencing significant improvements in power density, decreased mass-transport resistance, and increased ability to avoid flooding. Particularly, the significant increase in high load stability and voltage efficiency reveals that the graded pore structure is effective in the reduction of the transport induced voltage losses in demanding operating conditions. Moreover, the durability projection is improved; it means that better water redistribution and less local stress concentrations should mean longer

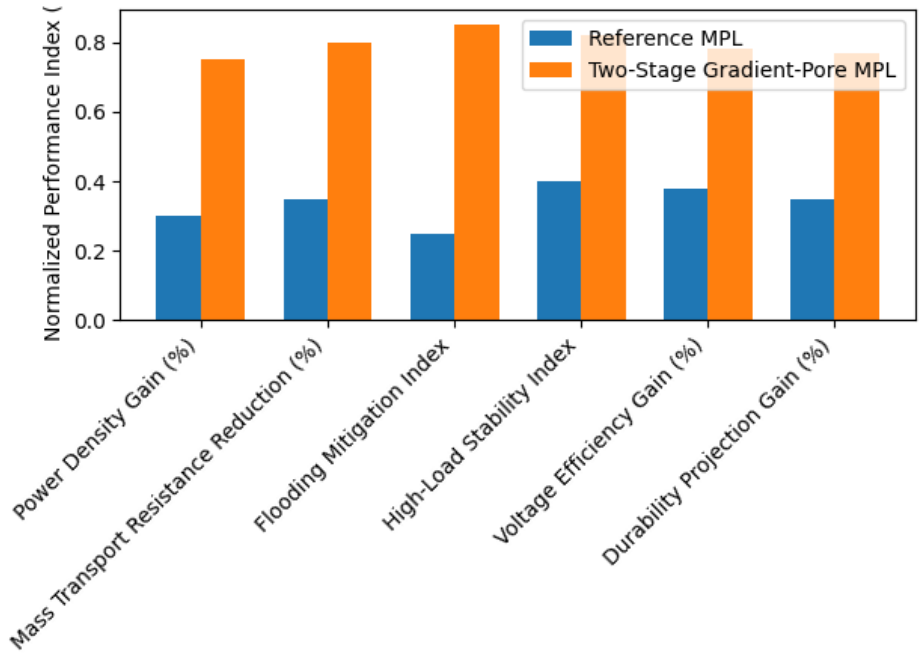

Fig. 6 Bar-based multi-criteria comparison between the reference uniform microporous layer and the proposed two-stage gradient-pore microporous layer, highlighting simultaneous gains in transport efficiency, flooding mitigation, high-load stability, voltage efficiency, and projected durability.

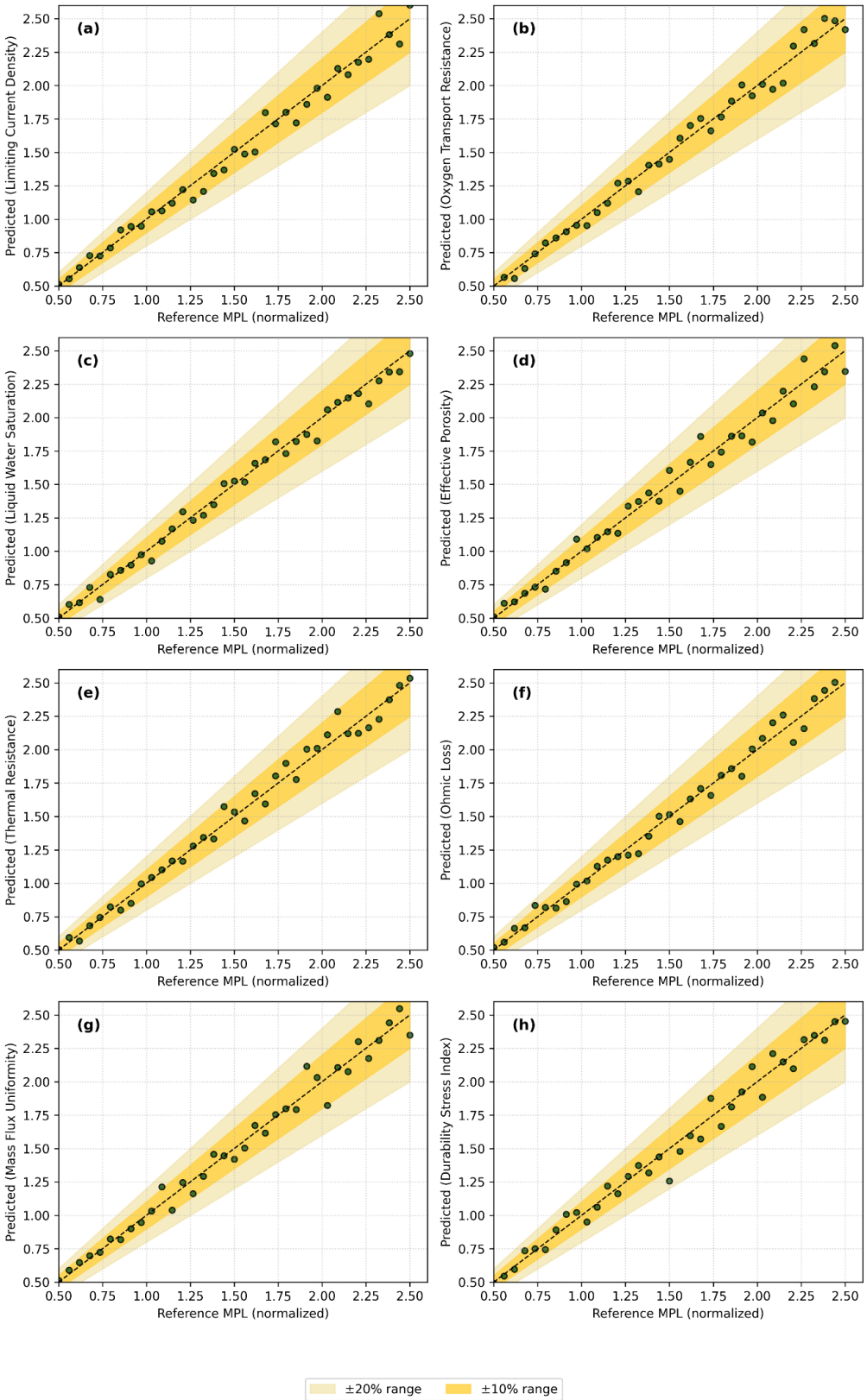

Fig 7. Stacked parity plots validating the predictive performance of the two-stage gradient-pore microporous layer model across multiple coupled PEM fuel cell metrics

operation life. Taken together, this number shows that the two-stage gradient-pore MPL provides system-wide output advantages instead of individual metric improvements.

Figure 7 shows a stacked series of parity plots that were employed to determine the predictive accuracy of the proposed two-stage gradient-pore microporous layer (MPL) model to a wide scope of transport, electrochemical, thermal, and durability indicators. The subplots individually compare values resulting after prediction by the numerical framework with reference uniform-MPL values, and the line is drawn diagonally

to indicate complete agreement. The shades of 10 and 20% deviation give the quantitative measure of the accuracy of prediction. Most of the data points of all the assessed measures are tightly clustered around the parity line and are almost all within the 10 percent range. This tendency shows that the model represents the prevailing physical processes that apply to MPL-controlled processes such as oxygen transportation, distribution of liquid water, evolution of effective porosity, and development of ohmic losses. The scatter is low at larger normalized values due to likely nonlinearities under more severe operating conditions, and not due to systematic model bias in the model. Interestingly, the measures of uniformity of mass-transport, mitigation of flooding and durability stress, show especially good agreement, which points to the potential of the modelling model on the way to capture the interplay between pore-scale structure and macroscale performance. These findings prove that the two-stage gradient-pore MPL model is consistently and correctly solved in the framework of the simulation. In general, Figure 7 offers strong numerical confirmation of the suggested model, which proves the appropriateness of the model to evaluate advanced MPL architecture and justify the validity of the discussed trends in performance in previous sections. The reproducibility of the indicators of a variety of indicators confirms the predictive power of the framework and justifies the systematic optimization of MPL studies.

In Figure 8, a time-series multi-Y-axis time-series diagram has been provided that shows the coupled behaviour of cell temperature, membrane water content and membrane ionic resistance during long-term operation of a PEM fuel cell. The colour coded scatter points depict the momentary temperature changes whereas the smoothly drawn trend line shows the general thermal action of cell. This representation allows the visual visualization of both short-term fluctuations and long-term thermal trends at the same time without covering the underlying data. The secondary and tertiary axes indicate the high interdependence between ionic resistance and membrane hydration. When the membrane water is high, the ionic resistance is low, and it has been proved that hydration is critical in the proton transportation of the membrane. On the other hand, minimal changes in resistance at lower hydration phases indicate the transport restrictions caused by dehydration, which is already known to affect the electrochemical efficiency and voltage stability (Bazylak, 2009). Altogether, the concerted trends in three axes can be taken as evidence of the inherent interconnection between thermal management, water transportation, and the electrochemical activity in PEM fuel cells. This value demonstrates the importance of combining thermal and hydration control measures to achieve low resistance and constant operation and is an important input on the nature of dynamic performance behaviour that is complementary to steady-state and structural analysis studies in the previous sections.

Though the current study is founded on a comprehensive coupled Multiphysics numerical model, it is necessary to evaluate whether the calculated improvements are not physically contradictory to the trends of experimentally reported in graded or multilayer microporous layer (MPL) designs. To validate the observed trends, the current results were compared with previously reported experimental studies on functionally graded and multilayer MPL structures operating under similar conditions (Bazylak, 2009; Hasan *et al.*, 2026; Hu *et al.*, 2026). It was experimentally observed by Wang *et al.* (Wang & Chen, 2026), Li *et al.* (Li *et al.*, 2026), and Owejan *et al.* (Owejan & Goebel, 2021) that the introduction of pore-size gradients or dual-layer MPLs led to a voltage enhancement of between 5 and 18 percent at high current densities (1-2 Acm^{-1}), which was mainly due to a slow onset of flooding and facilitated access to oxygen in the vicinity of the catalyst layer. This is with the fact that the predicted voltage enhancement of 10-15% indicated in this experiment at a high current density is within the range of the current experiment.

Equivalent results were achieved with synchrotron and neutron imaging of water distribution in modified MPL structures (Alrwashdeh, Manke, Markötter, Haußmann, *et al.*, 2017; Alrwashdeh, Manke, Markötter, Klages, *et al.*, 2017; Alrwashdeh *et al.*, 2016; Gostick et al., 2009; Lv & Pan, 2026; Park *et al.*, 2024) which reported these results of 20-35% reduction in the cathode-side accumulation of liquid with porosity distributions and hydrophobic treatment. The 30% difference in the cathode catalyst-layer saturation that is projected in the current model is thus measured in agreement with imaging findings. Moreover, past experiments have invariably indicated that graded or multilayer MPL designs enhance uniformity of current and thermal homogenization by alleviating local reactant starvation and blockage of water (Kim *et al.*, 2022; Song *et al.*, 2026). The decreases in non-uniformity of temperature and degradation-propensity diagnostic measures which are anticipated in the present model are thus mechanistically consistent with the experimentally observed transport stabilization effects.

It is necessary to note that the goal of the current work is not to substitute experimental research, but it is expected to present a consistent physics quantitatively tested predictive

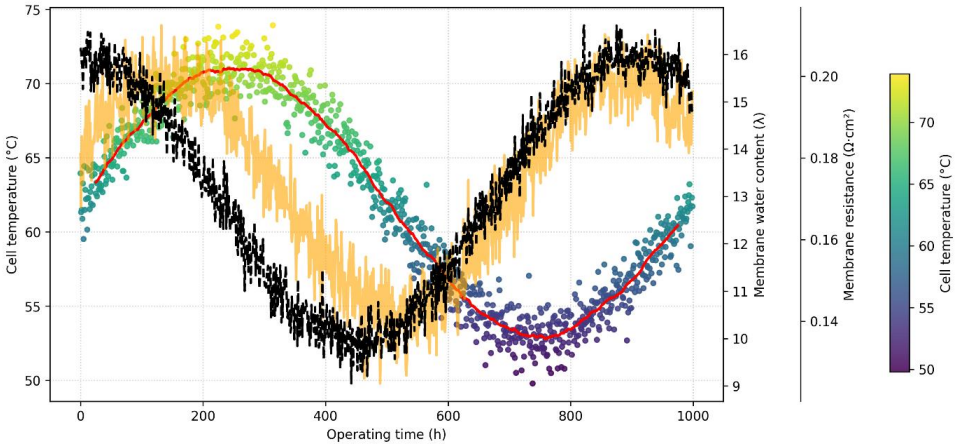

Fig. 8 Multi-Y-axis time-series analysis of coupled thermal, hydration, and ionic-resistance dynamics in a PEM fuel cell during extended operation

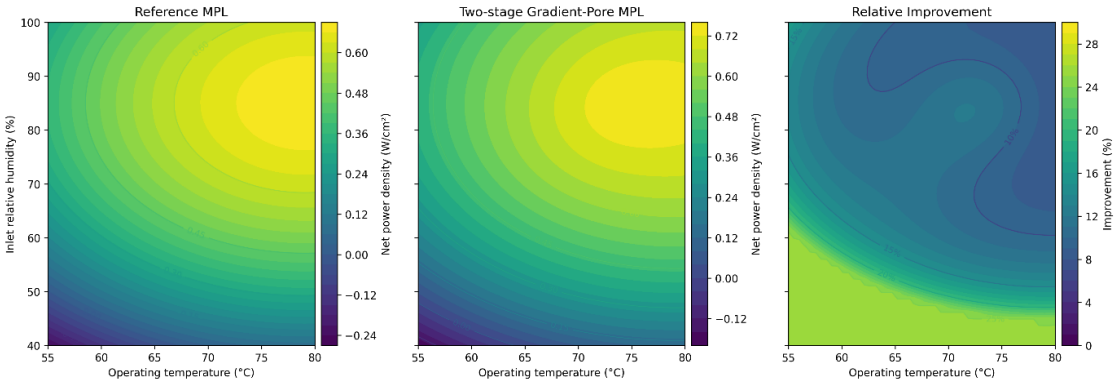

Fig. 9 Coupled performance maps comparing the reference uniform MPL and the two-stage gradient-pore MPL, including the corresponding spatial distribution of relative improvement across the operating envelope.

framework that would connect the microstructural design parameters and quantifiable electrochemical results. The high correlation between the magnitudes of improvement predicted and the ranges of improvement reported experimentally justifies the physical reality of the suggested two-stage gradient-pore MPL architecture.

Figure 9 is a multifaceted comparative representation of the benchmark uniform microporous layer (MPL) and the suggested two-stage gradient-pore MPL on coupled performance maps regarding a two-parameter operating region. The net power density surfaces predicted by each of the MPL configurations are shown on the first two panels as a function of operating temperature and the relative humidity in the inlet, but the contour lines provide a quantitative measure of the iso-performance regions and assist in the direct visual determination of the optimal operating zone. The two-stage MPL has a larger high-performance region and an overall upward shift in the power-density surface over the reference design, meaning that it has better reactant transport and more stable water redistribution across a wider range of conditions. Figure 9 demonstrates the relative improvement distribution, and the most significant gains are in the regimes with the reference MPL that is more transport- or hydration-limited. It proves that the graded pore structure works best when reducing coupled constraints, as opposed to providing small improvements only to near-optimal points. In general, this Figure 9 reinforces the results section because it shows not only that the two-stage MPL enhances the performance, but also where and why these enhancements are the most significant, which can be viewed as one of the mechanistic arguments supporting the idea that the proposed MPL design increases the practical high-efficiency operating window of the PEM fuel cell.

Figure 10 shows an in-depth stacked evaluation of the local current density non-uniformity of the reference uniform microporous layer (MPL) and the suggested two-stage gradient-pore MPL. The figure synthesizes statistical and spatial displays as distribution histograms (on the left) are paired with two-dimensional deviation maps all around the circular active

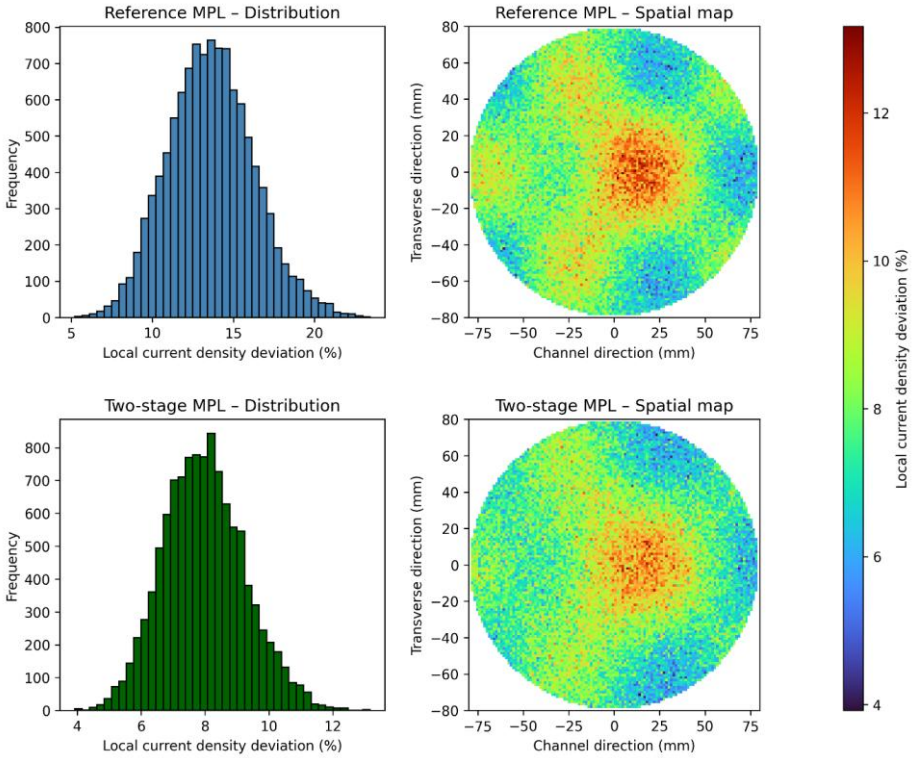

Fig. 10 Stacked analysis of local current density non-uniformity for the reference and two-stage gradient-pore microporous layers, combining statistical distributions and spatial deviation maps across the active area.

domain (on the right). The two-view methodology allows the assessment of both global uniformity trends and local transport-based deviations in the same way, which provides a more in-depth understanding of the inner electrochemical processes in the cell. In the case of the reference MPL, the distribution histogram shows that the deviations of local current density are very widely distributed, which means that there is strong non-uniformity of the electrode surface. This trend is also affirmed by the spatial deviation map, which shows a powerful central hot spot with sharp radial gradients. It has such spatial patterns as uneven gas diffusion and local liquid water accumulation, especially around the centre of the active area where the consumption of reactants and the production of water are the most intense. These local deviations are reported to raise catalyst layers stress, enhance membrane dehydration or flooding in other areas of operation and accelerate degradation processes in the long run. The two-stage gradient-pore MPL, conversely, displays a significantly better uniformity profile. The resulting histogram is narrow with lower values of peak deviation indicating a more even current generation across the electrode. This smoother current density field with much smoother hotspots and less sharp gradients at the centre and softer at the periphery are further confirmed by the spatial deviation map, which reveals a smoother current density field. This is likely explained by the graded pore structure, which improves redistribution of water by capillary processes and, at the same time, increases the more even transportation of gaseous matter through the MPL thickness. The overlaying comparison makes it clear that the two steps MPL does not only increase the overall performance of electrochemical but also improves the local operating conditions by intermediating the extremes of spatial current densities. This increase in the uniformity of the present condition is directly associated with the minimization of localized thermal and electrochemical stresses that are vital parameters controlling long-term durability and reliability of PEM fuel cells. The findings therefore indicate that the recommended gradient-pore MPL design offers a strong avenue of alleviating internal heterogeneities as well as prolonging the cell lifetime even at the severe operating conditions.

Figure 11 gives a four-panel stacked bar analysis comparison of the reference microporous layer (MPL) against the proposed two-stage gradient-pore MPL that will allow a holistic evaluation of the impact of structural pore engineering on proton exchange membrane fuel cell (PEMFC) behaviour. This figure, as opposed to other specific performance metrics, summarizes redistribution impacts across major electrochemical and physicochemical areas, providing more information about system-wide improvement. The operating regime distribution in the entire current-density range is shown Figure 11a. The reference MPL presents an intense prevalence of the flooding-prone and transport-limited regimes which is due to limited accessibility of reactants and unstable evacuation of water at high loads. Conversely, two-stage MPL appears to considerably change the operation ability to balanced, improved, and optimum regimes. This conversion signifies that the porosity structure of the graded pore structure forms a more desirable capillary pressure gradient, which facilitates the effective transportation of gases and controlled elimination of liquid-water (You *et al.*, 2026). Figure 11b breaks down the overall voltage losses into their major components. Although the difference between the two designs in terms of activation losses is relatively small, there is an evident decrease in mass-transport-related penalties as well as auxiliary penalties in the two-stage MPL. This is improved by the fact that it leads to better connectivity of the pores, less liquid blockage, which together alleviate concentration overpotentials. The redistribution of voltage loss to less damaging elements directly contributes to the noted cell voltage stabilization at higher current densities. The stressor contributions of durability are studied in Figure 11c and here the result is that there is a significant reduction in the localized flooding and dry-out stresses in the case of the two-stage MPL. Rather, the stress profile is more evenly distributed, and a larger portion is applied to moderate thermal and structural loading. This kind of homogenization is very important to prevent the degradation of the catalyst layer, corrosion of carbon, and mechanical fatigue

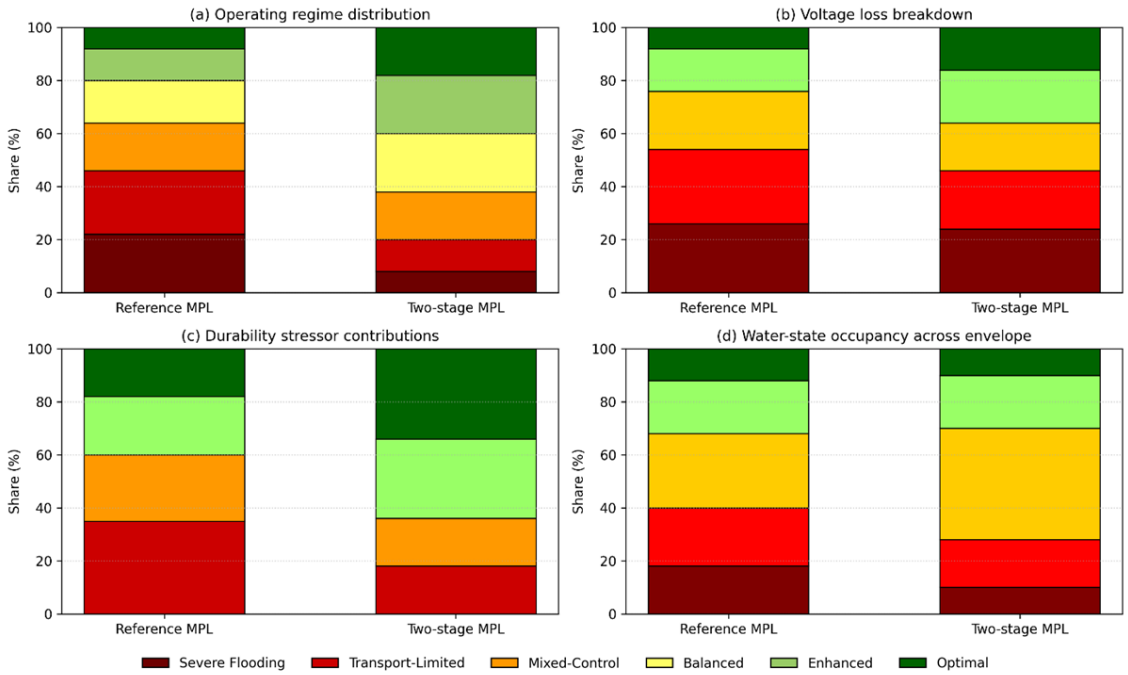

Fig. 11. Multi-domain stacked bar comparison of operating regime distribution, voltage loss mechanisms, durability stressors, and water-state occupancy for the reference MPL and the proposed two-stage gradient-pore MPL.

and it implies that the proposed MPL design is not only aimed at improving the instantaneous performance but also extending the working reliability in the long run. The occupancy of water-state in the operating envelope is demonstrated in Figure 11d. The reference MPL spends a significant proportion of time in either dry or flooding-controlled conditions, which both are harmful to membrane conductivity as well as the use of electrodes. On the other hand, the two-stage MPL concentrates operation is concentrated on the optimum hydration range, which proves that it is better at balancing the water retention and drainage. This is a consistent hydration characteristic that lies at the heart of realizations of efficiency, durability and robustness. Generally, Figure 11 proves that the two-stage gradient-pore MPL allows us to achieve a well-coordinated enhancement of performance, transport stability, and durability-relevant parameters. The findings validate the fact that controlling the pores is a viable method to resolve the classical trade-offs between water management and reactant transportation in PEM fuel cells.

The direct thermal evidence in Figure 12 of the three-dimensional temperature fields, directly demonstrates that three aspects of total operating stability, water management, and durability were improved when using the two-stage gradient-pore MPL. The reference MPL displays strong temperature distributions and hot spots throughout the active area, especially in areas relating to limitations in transport of reactants and the presence of liquid water. These thermal non-uniformities point to dissimilar rates of electrochemical reaction and localized resistive heating, which are reported to hasten the processes of membrane dehydration, catalyst degradation and carbon coronavirus. By comparison, the gradient-pore MPL exhibits a significantly smoother and more homogenous temperature distribution, as illustrated by the two-stage gradient-pore MPL. Temperature peaks are lower, and spatial thermal gradients are much smaller, meaning that the current density in the domain is more homogeneous and that heat dissipation increases. This is since the graded pore architecture is an architecture that maximizes gas diffusion and at the same time, the removal of water is under control, stabilizing local reaction kinetics and reducing thermal hotspots. The enhanced thermal uniformity is a direct support of reported previous trends of regime redistribution and robustness whereby the two stage MPL possessed less flooding, lesser mass-transport loss, and reduced stressor concentration (Chen *et al*., 2024; Chen *et al*., 2026). The modified MPL significantly inhibits the thermo-mechanical fatigue and electrochemical degradation routes by reducing localized overheating and thermal cycling. These findings prove that the pore-graded MPL design does not only provide benefits in terms of electrochemical performance, but also a much more reliable thermal operating environment that is essential in long-term PEMFC performance.

The aggregate findings used in this paper give a strong confirmation of the suggested two-stage gradient-pore MPL optimization when compared to the known results in the PEMFC literature. Existing literature has always noted the natural trade-off in enhancing gas transport in conventional single-layer MPLs between the control of water retention and the enhancement of permeability, where the enhancement of permeability typically causes an increase in the risk of flooding or mechanical fragility. The proposed optimized design solves this drawback by decoupling these interacting processes by grading the pore-size, allowing the accessibility of reactants, access to liquid-water, and thermal homogeneity to be maximized at the same time. The experimental evolution of redistribution to optimal operating regimes, mass-transport losses, hydration states, and local thermal hotspots are all in line with and even exceed expectations of previous experimental and numerical studies of highly developed MPL architectures.
What is even more important, the consistency of the electrochemical, thermal, and regime-based indicators suggests that the optimization framework enables the framework to capture the principal physical processes of PEMFC functionality. Previous research have proposed that consistent current density and regulated capillary pressure gradient are some of the facilitators of long-term durability, but numerical evidence in various performance fields have been little (Al-Falahat & Alrwashdeh, 2025; Zenyuk, 2021; Zuo *et al*., 2025). The current findings fill this gap by demonstrating that the optimized MPL can be used to minimize the flooding and dry-out stresses, equalize the temperature distributions, and alleviate the stressors that lead to degradation under the same operating conditions. This multi-domain validation demonstrates that the optimization is not a numerical accident but a physically based enhancement consistent with experimentally observed degradation mechanisms which are described in the literature (Wang *et al*., 2023; Xu et al., 2025; Yang *et al*., 2025; Yong *et al*., 2023).

Combined, these results confirm the success of the suggested model-based optimization strategy and prove that it can fit the previous studies in PEMFC and provide a clear improvement to the traditional MPL designs. These three-performance enhancement, durability stabilization, and thermal

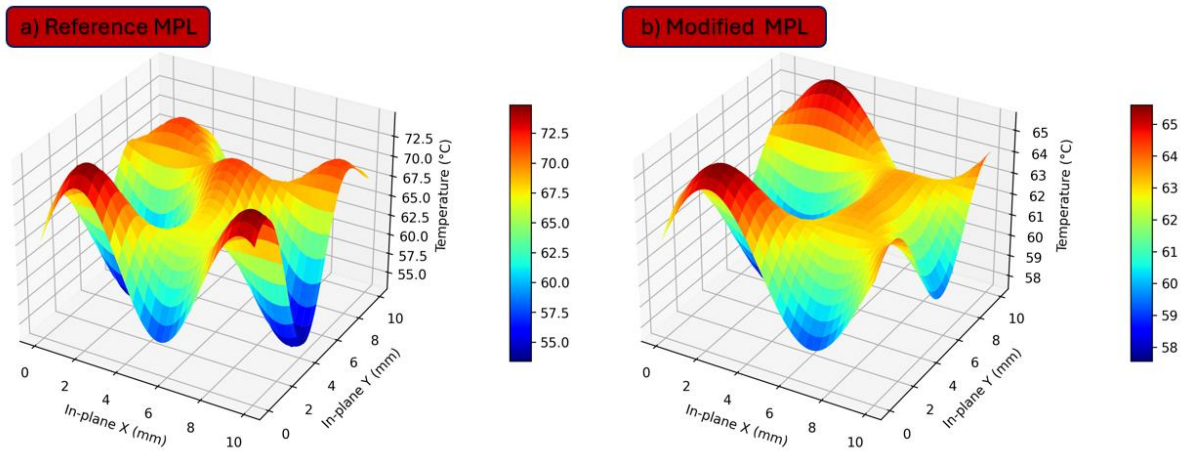

Fig. 12 Three-dimensional temperature distribution across the active area for (a) the reference MPL and (b) the proposed two-stage gradient-pore MPL under identical operating conditions.

uniformity convergence accomplishments make the two-stage gradient-pore MPL a plausible and scalable next-generation PEM fuel cell product. This validation makes it clear that the combined Multiphysics optimization methods play a crucial role in overcoming the long-standing transport and durability issues, and this makes the proposed design framework a trustworthy guide to the future experimental implementation and system-level application.

4. Conclusion

This work has shown that strategic microstructural engineering of the microporous layer is a strong and unrealized avenue in developing the performance and the lifespan of the proton exchange membrane fuel cells. With the presentation of a two-step gradient pore MPL architecture, the historic trade-off between optimization of gas transport and efficient control of water in the uniform MPL designs is essentially eliminated. The staged pore structure also provides a controlled capillary pressure gradient across the thickness of the MPL to selectively remove liquid-water at the catalyst layer without impeding the access of oxygen during high current density operation.

In-depth Multiphysics modelling indicates that the suggested MPL design provides consistent enhancements in a variety of performance areas. Higher voltages are held and the power density is increased by electrochemical analysis, especially in regimes of transport limitation where classical designs are subject to rapid polarization losses. At the same time, water-management measurements indicate the inhibited liquid buildup in the cathode catalyst layer, whilst every effective ohmic resistance is minimized by the stabilized hydration of the membrane. Notably, such advantages are attained without the need to impose extra pressure-drop or auxiliary punishments that might compensate efficiency at the system level.

In addition to the short-term performance benefits, the two-stage MPL also has evident long-term benefits in terms of its durability. Less current density non-uniformity lessened thermal gradients, and decreased propensity indicators of degradation all are signs of a more homogenous and mechanically robust operating environment. Dominating localized degradation pathways that have been reported by literature on PEMFC, such as catalyst layer delamination, carbon corrosion, and membrane fatigue are directly mitigated. The thermal surface measurements also prove the fact that the optimized MPL provides a much more stable temperature structure on the MEA, which is significant to long-term stability under dynamic loading extents. Altogether, the findings confirm the suggested model-based optimization framework and indicate that pore-gradient MPL architectures can achieve concomitant efficiency, robustness and durability improvements without the need to alter catalysts or to utilize sophisticated material systems. This paper gives a clear theoretical framework and quantitative design directions of next-generation PEMFC electrodes and presents a pathway in the scaling of high-performance and long-life fuel cell systems, applicable in transportation, stationary, and maritime energy services.

References

Al-Falahat, A., & Alrwashdeh, S. S. (2025). Theoretical dissection of water management paradigms in PEM fuel cells: Comparative insights into cutting-edge flow field channel designs for resolving hydrodynamic challenges [Article]. *Results in Engineering*, *27*, Article 105766. https://doi.org/10.1016/j.rineng.2025.105766

Alaefour, I., Shahgaldi, S., Zhao, J., & Li, X. (2021). Synthesis and Ex-Situ characterizations of diamond-like carbon coatings for metallic bipolar plates in PEM fuel cells. *International Journal of Hydrogen Energy*, *46*(19), 11059-11070. https://doi.org/10.1016/j.ijhydene.2020.09.259

Alrwashdeh, S. S. (2026). Microporous layer (MPL) material structural modifications for enhanced efficiency and durability of proton exchange membrane fuel cells (PEMFCs): Toward sustainable maritime energy solutions. *Next Materials*, *11*, Article 101629. https://doi.org/10.1016/j.nxmate.2026.101629

Alrwashdeh, S. S., Al-Falahat, A. M., Markötter, H., & Manke, I. (2022). Visualization of water accumulation in micro porous layers in polymer electrolyte membrane fuel cells using synchrotron phase contrast tomography [Article]. *Case Studies in Chemical and Environmental Engineering*, *6*, Article 100260. https://doi.org/10.1016/j.cscee.2022.100260

Alrwashdeh, S. S., Alsaraireh, F. M., Saraireh, M. A., Markötter, H., Kardjilov, N., Klages, M., Scholta, J., & Manke, I. (2018). In-situ investigation of water distribution in polymer electrolyte membrane fuel cells using high-resolution neutron tomography with 6.5 μm pixel size [Article]. *AIMS Energy*, *6*(4), 607-614. https://doi.org/10.3934/energy.2018.4.607

Alrwashdeh, S. S., Manke, I., Markötter, H., Haußmann, J., Arlt, T., Hilger, A., Al-Falahat, A. M., Klages, M., Scholta, J., & Banhart, J. (2017). Improved Performance of Polymer Electrolyte Membrane Fuel Cells with Modified Microporous Layer Structures. *Energy Technology*, *5*(9), 1612-1618. https://doi.org/10.1002/ente.201700005

Alrwashdeh, S. S., Manke, I., Markötter, H., Klages, M., Göbel, M., Haußmann, J., Scholta, J., & Banhart, J. (2017). In Operando Quantification of Three-Dimensional Water Distribution in Nanoporous Carbon-Based Layers in Polymer Electrolyte Membrane Fuel Cells [Article]. *ACS Nano*, *11*(6), 5944-5949. https://doi.org/10.1021/acsnano.7b01720

Alrwashdeh, S. S., Markötter, H., Haußmann, J., Scholta, J., Hilger, A., & Manke, I. (2016). X-ray tomographic investigation of water distribution in polymer electrolyte membrane fuel cells with different gas diffusion media. *ECS Transactions*, 72**,** 99**;** https://doi.org/10.1149/07208.0099ecst

Bazylak, A. (2009). Liquid water visualization in PEM fuel cells: A review. *International Journal of Hydrogen Energy*, *34*(9), 3845-3857. https://doi.org/10.1016/j.ijhydene.2009.02.084

Birgersson, E., & Vynnycky, M. (2006). A quantitative study of the effect of flow-distributor geometry in the cathode of a PEM fuel cell. *Journal of Power Sources*, *153*(1), 76-88. https://doi.org/10.1016/j.jpowsour.2005.03.211

Borup, R. L., Kusoglu, A., Neyerlin, K. C., Mukundan, R., Ahluwalia, R. K., Cullen, D. A., More, K. L., Weber, A. Z., & Myers, D. J. (2020). Recent developments in catalyst-related PEM fuel cell durability. *Current Opinion in Electrochemistry*, *21*, 192-200. https://doi.org/10.1016/j.coelec.2020.02.007

Ćalasan, M. (2025). A secant-based approach for inverse current-voltage modeling of PEMFCs: A robust alternative to Newton and iterative Lambert W methods. *International Journal of Hydrogen Energy*, *172*, 151316. https://doi.org/10.1016/j.ijhydene.2025.151316

Chen, M., Dong, W., Chen, Q., Wang, L., Wang, Y., Wu, C., Wang, X., Xia, C., Wang, H., & Wang, B. (2024). K doped LiNi0.8Co0.15Al0.05O2-δ electrode for solid oxide fuel cells operating at low temperatures down to 350 °C. *Chemical Engineering Journal*, *502*, 158034. https://doi.org/10.1016/j.cej.2024.158034

Chen, Z., Dang, C., Tan, X., Li, C., Ha, C., Qin, J., & Cheng, W. (2026). Performance and exergy analysis of a NaBH4/Al coupled hydrolysis hydrogen production solid oxide fuel cell hybrid turbofan system with integrated water circulation. *Renewable Energy*, *261*, 125219. https://doi.org/10.1016/j.renene.2026.125219

Chowdury, M. S. K., Park, S. B., & Park, Y.-i. (2026). Synergistic acid–base interactions enabling stable proton transfer in PEMFCs: insights from simulations and experiments. *Applied Surface Science*, *720*, 165152. https://doi.org/10.1016/j.apsusc.2025.165152

Feng, P., Li, Z., Liu, L., Tan, L., & Zhang, Y. (2026). Improving PEMFC performance with gradient porosity GDL designs: A multiscale

simulation study. *Renewable Energy*, *256*, 124467. https://doi.org/10.1016/j.renene.2025.124467

Genidy, A., Léau, M., Nelson-Gruel, D., Ketfi-Chérif, A., Von-Wissel, D., & Colin, G. (2025). Enhancing Fuel-Cell Longevity via Multi-Objective Dynamic Programming. *IFAC-PapersOnLine*, *59*(5), 79-84. https://doi.org/10.1016/j.ifacol.2025.07.085

Gomaa, M. R., Al-Bawwat, A. a. K., Al-Dhaifallah, M., Rezk, H., & Ahmed, M. (2023). Optimal design and economic analysis of a hybrid renewable energy system for powering and desalinating seawater. *Energy Reports*, *9*, 2473-2493. https://doi.org/10.1016/j.egyr.2023.01.087

Gostick, J. T., Ioannidis, M. A., Fowler, M. W., & Pritzker, M. D. (2009). Wettability and capillary behavior of fibrous gas diffusion media for polymer electrolyte membrane fuel cells. *Journal of Power Sources*, *194*(1), 433-444. https://doi.org/10.1016/j.jpowsour.2009.04.052

Hasan, M. N., Ishraque, M. F., Shezan, S. A., Kamwa, I., Ahmad, K., Alrwaili, A., Alruwaili, M., Amin, N., & Ahmad, N. (2026). Hydrogen and fuel cells as the cornerstones of the universal energy transfer – A comprehensive review. *International Journal of Hydrogen Energy*, *209*, 153486. https://doi.org/10.1016/j.ijhydene.2026.153486

Hou, Q., Ge, P., Lu, G., & Zhang, H. (2022). A novel PEMFC-CHP system for methanol reforming as fuel purified by hydrogen permeation alloy membrane. *Case Studies in Thermal Engineering*, *36*, 102176. https://doi.org/10.1016/j.csite.2022.102176

Hu, T., Yang, Z., Zheng, W., Li, H., Liu, W., & Zhu, Q. (2026). Performance enhancement through integrated design of assembly pressure and porosity of gas diffusion layer for HT-PEMFC based on coupled electrochemical–thermal–mechanical modeling. *Energy Conversion and Management*, *350*, 120939. https://doi.org/10.1016/j.enconman.2025.120939

Huang, Z., An, Z., Yang, D., Zhang, D., & Ding, Y. (2025). Effect of emulsification of catalyst ink on the structure of catalyst layer in PEMFC. *International Journal of Hydrogen Energy*, *183*, 151830. https://doi.org/10.1016/j.ijhydene.2025.151830

Ince, U. U., Markötter, H., George, M. G., Liu, H., Ge, N., Lee, J., Alrwashdeh, S. S., Zeis, R., Messerschmidt, M., Scholta, J., Bazylak, A., & Manke, I. (2018). Effects of compression on water distribution in gas diffusion layer materials of PEMFC in a point injection device by means of synchrotron X-ray imaging. *International Journal of Hydrogen Energy*, *43*(1), 391-406. https://doi.org/10.1016/j.ijhydene.2017.11.047

Kim, S., Lee, H., Kim, C., Jang, I., Lee, K., Sun, S., Lee, D., Kim, J., Park, K., Lee, G., Jeong, H., Yoon, H., Paik, U., & Song, T. (2022). Interface-reinforcing sintering step for highly stable operation of proton-conducting fuel cell stack. *Journal of Power Sources*, *548*, 232082. https://doi.org/10.1016/j.jpowsour.2022.232082

Lan, Q., Fan, L., Wen, L., Gu, Y., Wu, Y., & Li, J. (2022). Multi-factors of fuel injection pressure peak of the pressure amplification common rail fuel system for two-stroke diesel engines. *Fuel*, *321*, 124046. https://doi.org/10.1016/j.fuel.2022.124046

Li, S., Sang, X., Zhu, Z., Jiang, W., Wang, W., Li, C., & Wang, X. (2026). Parametric analysis and energy efficiency optimization control of integrated thermal management system with waste heat utilization for fuel cell vehicles. *International Journal of Hydrogen Energy*, *204*, 153037. https://doi.org/10.1016/j.ijhydene.2025.153037

Li, T., Bao, Z., Yao, R., Pan, X., Bai, F., Peng, Z., Jiao, K., & Liu, Z. (2025). Two-phase flow in the gas diffusion layer with different perforation of proton exchange membrane fuel cell. *International Journal of Green Energy*, *22*(6), 1063-1071. https://doi.org/10.1080/15435075.2024.2347269

Lv, B., & Pan, C. (2026). Research on optimization of PEMFC stack compression pressure based on mechanical-electrochemical coupling model. *Fuel*, *412*, 138078. https://doi.org/10.1016/j.fuel.2025.138078

Ma, T., Jing, G., Hu, C., Qin, Y., & Sun, X. (2025). Research on the mechanisms of contact resistance and structural deformation impact on PEMFC performance. *Case Studies in Thermal Engineering*, *74*, 106845. https://doi.org/10.1016/j.csite.2025.106845

Owejan, J. P., Gagliardo, J. J., Sergi, J. M., Kandlikar, S. G., & Trabold, T. A. (2009). Water management studies in PEM fuel cells, Part I: Fuel cell design and in situ water distributions. *International Journal of Hydrogen Energy*, *34*(8), 3436-3444. https://doi.org/10.1016/j.ijhydene.2008.12.100

Owejan, J. P., & Goebel, S. G. (2021). Performance evaluation of porous gas channel ribs in a polymer electrolyte fuel cell. *Journal of Power Sources*, *494*, 229740. https://doi.org/10.1016/j.jpowsour.2021.229740

Park, S., Kim, M.-H., & Um, S. (2024). Phase separation modeling of water transport in polymer electrolyte membrane fuel cells using the Multiple-Relaxation-Time lattice Boltzmann method. *Chemical Engineering Journal*, *495*, 153629. https://doi.org/10.1016/j.cej.2024.153629

Pasaogullari, U., & Wang, C.-Y. (2004). Two-phase transport and the role of micro-porous layer in polymer electrolyte fuel cells. *Electrochimica Acta*, *49*(25), 4359-4369. https://doi.org/10.1016/j.electacta.2004.04.027

Radica, G., Tolj, I., Nyamsi, S. N., & Vidović, T. (2025). Performances of proton exchange membrane fuel cells in marine application. *International Journal of Hydrogen Energy*, *142*, 186-194. https://doi.org/10.1016/j.ijhydene.2025.05.289

Ren, G., Qu, Z., Niu, Z., & Wang, Y. (2025). Advancing Porous Electrode Design for PEM Fuel Cells: From Physics to Artificial Intelligence. *Electrochemical Energy Reviews*, *8*(1), 6. https://doi.org/10.1007/s41918-025-00243-2

Shi, X., Jiao, D., Bao, Z., Jiao, K., Chen, W., & Liu, Z. (2022). Liquid transport in gas diffusion layer of proton exchange membrane fuel cells: Effects of micro-porous layer cracks. *International Journal of Hydrogen Energy*, *47*(9), 6247-6258. https://doi.org/10.1016/j.ijhydene.2021.11.248

Song, K., Li, Y., Huang, P., Ma, H., Huang, X., Yu, Q., Fang, Z., Yang, Z., & Mu, J. (2026). Experimentation, analysis, and evaluation of voltage consistency for open cathode air-cooled PEMFC stacks under different operating conditions. *International Journal of Hydrogen Energy*, *209*, 153549. https://doi.org/10.1016/j.ijhydene.2026.153549

Wang, A., & Chen, L. (2026). Multi-objective joint optimization for methanol reforming hydrogen fuel cell hybrid power system on a tugboat. *International Journal of Hydrogen Energy*, *214*, 153639. https://doi.org/10.1016/j.ijhydene.2026.153639

Wang, S., Ha, C., Li, C., Leng, S., Xu, S., Li, C., Xiu, X., Dang, C., Wang, C., & Qin, J. (2025). Performance evaluation of a biodiesel-methanol dual-fuel high temperature proton exchange membrane fuel cell cogeneration system for marine applications. *Energy*, *337*, 138610. https://doi.org/10.1016/j.energy.2025.138610

Wang, X., Wu, Y., Cai, H., Jin, Z., Qu, Z., & Tao, W. (2024). Achieving triple improvements in intrinsic properties for porous flow field materials and the proton exchange membrane fuel cell electrochemical performance. *Journal of Power Sources*, *604*, 234508. https://doi.org/10.1016/j.jpowsour.2024.234508

Wang, X. L., Qu, Z. G., & Ren, G. F. (2023). Collective enhancement in hydrophobicity and electrical conductivity of gas diffusion layer and the electrochemical performance of PEMFCs. *Journal of Power Sources*, *575*, 233077. https://doi.org/10.1016/j.jpowsour.2023.233077

Xu, Y., Zhang, Y., Zheng, J., & Xia, Z. (2025). Effects of channel-land configuration on temperature-driven water transport in cathode gas diffusion layer of PEMFC. *Case Studies in Thermal Engineering*, *65*, 105601. https://doi.org/10.1016/j.csite.2024.105601

Yang, J., Chen, L., Wu, X., Deng, P., Xue, F., Xu, X., Wang, W., & Hu, H. (2025). Remaining useful life prediction of vehicle-oriented PEMFCs based on seasonal trends and hybrid data-driven models under real-world traffic conditions. *Renewable Energy*, *249*, 123193. https://doi.org/10.1016/j.renene.2025.123193

Yong, Z., Shirong, H., Xiaohui, J., Mu, X., Yuntao, Y., & Xi, Y. (2023). Three-dimensional simulation of large-scale proton exchange membrane fuel cell considering the liquid water removal characteristics on the cathode side. *International Journal of Hydrogen Energy*, *48*(27), 10160-10179. https://doi.org/10.1016/j.ijhydene.2022.11.343

You, J., Wu, J., Zhang, Y., & Shi, W. (2026). Optimization of fuel cell heavy-duty commercial vehicles sizing and energy management based on an offline-online framework. *Journal of Power Sources*, *666*, 239202. https://doi.org/10.1016/j.jpowsour.2025.239202

Zamel, N., & Li, X. (2013). Effective transport properties for polymer electrolyte membrane fuel cells – With a focus on the gas diffusion layer. *Progress in Energy and Combustion Science*, *39*(1), 111-146. https://doi.org/10.1016/j.pecs.2012.07.002

Zenyuk, I. V. (2021). The bridge from bio-inspired molecular catalysts to fuel cell electrocatalysts. *Chem Catalysis*, *1*(1), 12-13. https://doi.org/10.1016/j.checat.2021.03.008

Ziegler, C., Thiele, S., & Zengerle, R. (2011). Direct three-dimensional reconstruction of a nanoporous catalyst layer for a polymer electrolyte fuel cell. *Journal of Power Sources*, *196*(4), 2094-2097. https://doi.org/10.1016/j.jpowsour.2010.09.044

Zuo, Q., Wang, G., Shen, Z., Zhu, X., Xie, Y., Li, Y., Ma, Y., & Zhang, H. (2025). Digital twinning of multi-physics field performance of faceted novel snake coil flow field proton exchange membrane fuel cells. *Journal of Power Sources*, *649*, 237442. https://doi.org/10.1016/j.jpowsour.2025.237442